

## Bursting of a thin film in a confined geometry: Rimless and constant-velocity dewetting

Ayako Eri and Ko Okumura\*

*Department of Physics, Graduate School, Ochanomizu University, 2-1-1, Otsuka, Bunkyo-ku, Tokyo 112-8610, Japan*  
(Received 24 June 2010; published 1 September 2010; corrected 14 September 2010)

We study the bursting dynamics of a thin oil film sandwiched by glycerol aqueous solution in a confined geometry where the circular symmetry of the bursting hole is broken. We find that the bursting proceeds with a constant velocity except for initial times and the velocity is governed by the viscosity of the surrounding glycerol. Different from previous studies where the bursting speed is constant, in our confined geometry no rims are formed at the bursting tip as a result of the symmetry breaking. Our findings can be explained by original and simple scaling arguments.

DOI: [10.1103/PhysRevE.82.030601](https://doi.org/10.1103/PhysRevE.82.030601)

PACS number(s): 68.15.+e, 47.55.df, 68.08.Bc

Bursting of liquid thin film has been studied for more than a century. This phenomenon is familiar to everybody as the rupture of soap films, and is important in many fields [1,2]: it is observed with polymer foams, emulsions, in glass furnaces, and during volcanic eruption, and plays a crucial role in many industrial processes including manufacturing nanodevices. Accordingly, it is still an active area of research and the effect of residual stress in the film is one of the current topics [3,4]. Although the fundamental physics of the dynamics of bursting film is rather well and simply understood [5], in all previous studies the bursting hole has circular symmetry and no knowledge is available in the literature when this symmetry is broken due to confinement. Here, we study for the first time bursting of a thin film in a confined geometry, which is relevant in many practical situations where small amount of liquids has to be manipulated (e.g., microfluidics and biological applications). As a result, we find a new physical regime of the bursting dynamics, which is potentially important in various practical contexts.

The fundamental physical understanding of film bursting pertinent to the present study can be categorized by the following four examples. (1) The bursting of soap film suspended in air proceeds with a constant speed where capillary drive balances with inertia (if the film is not extremely thin) [6–8]. (2) The bursting of liquid film on a solid substrate (i.e., dewetting) also proceeds with a constant speed where capillary drive balances with viscous dissipation inside the liquid [9]. (3) When a soap film is suspended in viscous oil phase, the bursting proceeds also at a constant speeds where capillary drive balances with viscous dissipation not inside the soap film but inside the surrounding oil phase [10]. In all three cases, the rim is formed at the bursting tip: the moving part of a bursting film is only the rim and the burst portion of film is all collected to the rim. (4) On the contrary, when a highly viscous film is suspended in air, the bursting speed of the viscous film grows with time and no rim is formed at the bursting tip [11,12]: as if a stretched elastic sheet shrank, the film thickness increases homogeneously due to the short-time viscoelastic (i.e., elastic) nature of entangled polymer melt [13].

In summary, the bursting or dewetting frequently pro-

ceeds with a constant speed and in such cases a rim is formed; when the rim is not formed the speed grows with time. On the contrary, in this study, we find a remarkable type of bursting, which proceeds with a constant speed but no rim is formed. This is because of a symmetry breaking due to the confined geometry as discussed below.

To realize a confined geometry, we use a Hele-Shaw cell of 10-cm dimensions made from two transparent acrylic boards of millimeter thickness [Fig. 1(a)], [14]. The boards are separated by a distance  $D$ , with acrylic spacers of homogeneous thickness. We fill the cell first with olive oil and then with glycerol (plus water). We dilute glycerol with water to change the viscosity below. Since the oil is lighter than the glycerol, after a while the oil layer is on top of the glycerol layer [Fig. 1(a)]. This order of filling guarantees the

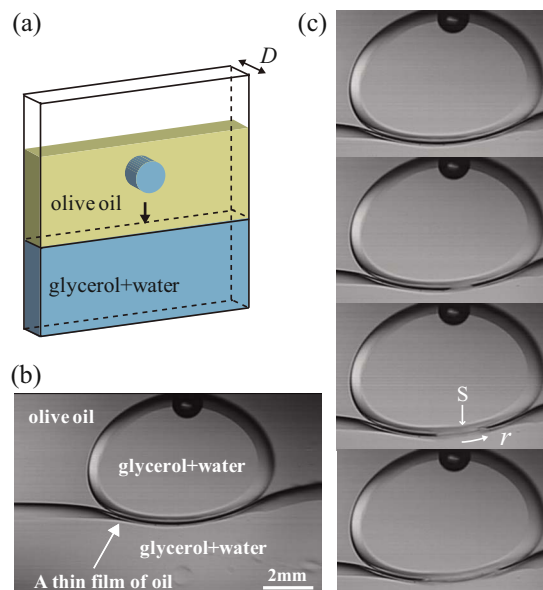


FIG. 1. (Color online) (a) Illustration of the experiment. (b) A glycerol droplet sitting at the oil-glycerol interface where a thin oil film underneath the droplet disallows coalescence typically for a few minutes. The white bar stands for the cell thickness  $D$  ( $\approx 2$  mm). (c) The dynamics of coalescence: bursting of a thin film of oil between the droplet and the bath. The snapshots are separated by 15/8000 s. The length  $r$  stands for the distance between the bursting tip and the point (indicated as S) where the bursting started.

\*Corresponding author; okumura@phys.ocha.ac.jp

existence of thin oil film between the cell plates and the glycerol layer to avoid direct contact of glycerol to the plates.

We then let a glycerol droplet fall down in the oil by gravity [Fig. 1(a)]. The droplet contains the same amount of water as the bulk phase. Again due to the existence of a thin oil film between the droplet and the cell plates, there is no direct contact of the droplet with the plates. When the glycerol droplet reaches the interface between oil and glycerol, a thin film of oil (of thickness  $h$ ) remains between the oil-glycerol interface to avoid an immediate coalescence of the droplet with the bulk phase [Fig. 1(b)]. The film (of thickness  $h$ ) survives typically for a few minutes until it suddenly bursts to initiate the coalescence [Fig. 1(c)]. In all cases, we waited till the bursting occurred spontaneously (the starting position of bursting was unpredictable).

We measured the distance ( $r$ ) of the bursting tip from the point where the bursting started [Fig. 1(c)] as a function of time from snapshots taken by a high speed camera (Nac fx6000). The results for different thicknesses,  $D=1$  mm and 2 mm, are summarized in Figs. 2(a) and 2(b), respectively, where viscosity is changed as specified in Table I. The origin of time,  $t=0$ , is defined as the moment when the bursting starts [the origin can be shifted at most 1/2000 s because the number of frame per second (here, from 2000 to 8000 fps) is not fast enough to capture the exact moment].

As shown in Fig. 2, the bursting tip advances at constant speed (though not perfect). In addition, the constant velocity clearly depends on the viscosity of glycerol aqueous solution ( $\eta_g$ ), which ranges from 12.7 to 316 mPa s, while that of olive oil ( $\eta_o$ ) is a constant, around 60 mPa s, throughout this study. This suggests that dissipation in the glycerol phase is important in this constant-velocity regime.

To understand the constant-velocity dynamics, we consider that this dynamics is governed by the interfacial drive opposed by a viscous friction. The interfacial energy decrease per unit time scales as  $\gamma DV$  while the viscous energy dissipation per unit time as  $\eta(V/l)^2\Omega$ . Here,  $V/l$  is the gradient of the bursting velocity and  $\Omega$  is the volume disturbed by the bursting. We expect that the dynamics is determined by balancing these quantities:  $\gamma DV \sim \eta(V/l)^2\Omega$ .

Our problem now boils down to estimate the appropriate scales of  $\eta$ ,  $l$ , and  $\Omega$ . For this purpose, we show a magnified snapshot of the bursting tips in Fig. 3(a). Here, we cannot recognize a rim of the type illustrated in Fig. 3(b), which is frequently seen at the tip of a bursting film (we can instead regard the present situation as if the rim size  $a$  were equal to the film thickness  $h$ ). This absence of rim is reasonable because the burst volume of the oil film can escape in the direction of cell thickness as illustrated in Fig. 3(c). The burst volume is not collected at the tip to form a rim as in frequently observed in previous studies; in all previous cases,

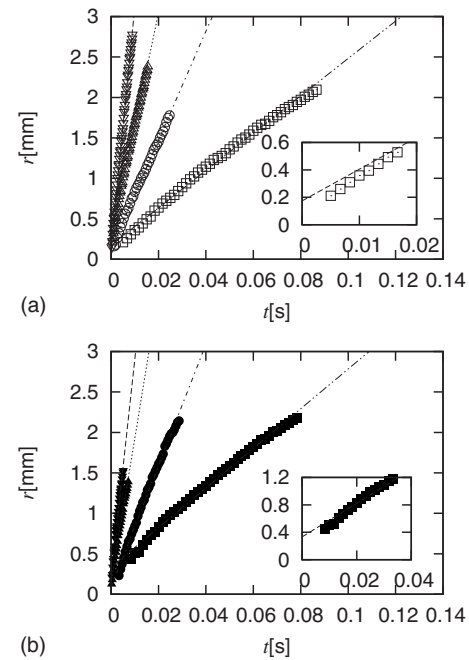


FIG. 2. Bursting tip position  $r$  as a function of time  $t$ . (a)  $D=1$  mm and (b)  $D=2$  mm. The straight lines fit the corresponding data sets. The insets magnify the initial dynamics for  $\eta_g=280$  mPa s in (a) and 316 mPa s in (b).

the growing hole has a circular symmetry: the symmetry along the direction perpendicular to the retracting direction is preserved so that this kind of escape dynamics is forbidden. The escape dynamics indicated in Fig. 3(c) associated with  $\eta_o$  is much slower than the bursting dynamics and extend over a scale rather larger than the film thickness  $h$  (but less than the cell thickness  $D$ ) as seen in Fig. 3(a) or Fig. 1(c). On the contrary, the faster bursting dynamics (characterized by a velocity  $V$ ) seems very localized. In other words, the dissipation in the surrounding glycerol can be estimated by assuming that a cylinder of radius  $h$  and of length  $D$  is moving, i.e.,  $l \sim h$  and  $\Omega \sim \pi h^2 D$ . This gives a dissipation (per time)  $\eta_g V^2 D$ . Since our experimental  $V$  strongly depends on  $\eta_g$  we first neglect the dependence on  $\eta_o$ . This implies that the dissipation in the surrounding glycerol dominates over that in the oil film. This assumption is further discussed below. Note here that thin oil films between the droplet and acrylic boards do not contribute to dissipation because the center of gravity of the droplet does not move during the bursting.

Under the above assumption, the dissipation in the glycerol  $\eta_g V^2 D$  is balanced with the capillary drive. In this way, we obtain the bursting velocity

TABLE I. Viscosity  $\eta_g$  of glycerol aqueous solution in Figs. 2 and 4. The viscosity of the oil is a constant around 60 times as viscous as water. The open and black marks correspond to  $D=1$  and 2 mm, respectively.

	▽	△	○	□	▼	▲	●	■
$\eta_g$ [mPa s]	13.9	53.1	125	280	12.7	40.2	128	316

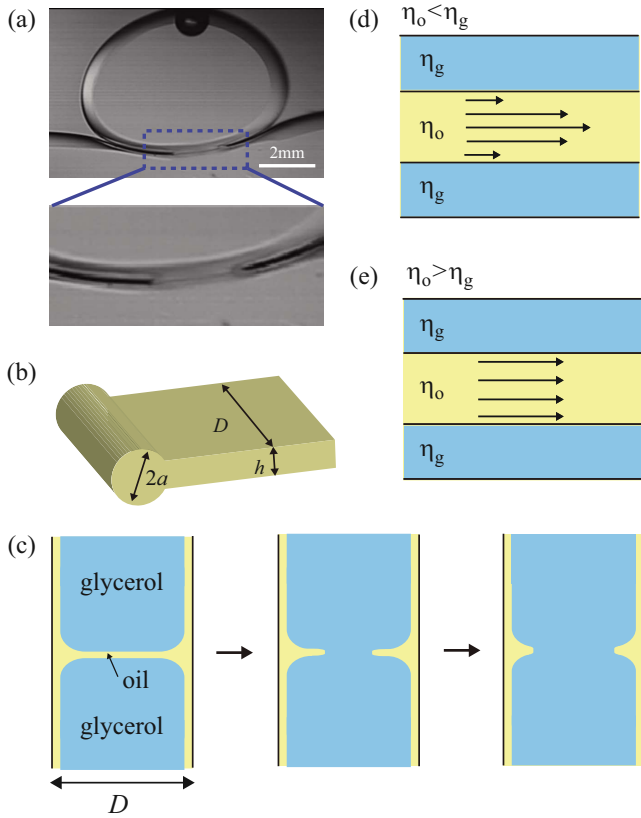


FIG. 3. (Color online) (a) Magnified snapshot of the bursting tips. The white bar stands for the cell thickness  $D$ . (b) Illustration of a rim (of size  $a$ ) frequently observed in the bursting of a film (but not observed in the present case). (c) Dynamical change of the section of burst film (side view). The two vertical lines indicate the surface of the cell plates which are separated by  $D$ . (d) Poiseuille flow. (e) Plug flow. In general, when a flowing thin film (o) is sandwiched by another fluid (g), the Poiseuille and plug flows develop for  $\eta_g \gg \eta_o$  and  $\eta_g \ll \eta_o$ , respectively.

$$V = \alpha \gamma / \eta_g. \quad (1)$$

Here,  $\alpha$  is the exact coefficient under the cylinder approximation [15]. This actually depends weakly on  $V$  and is given by  $l/(2\pi)$  where

$$l \approx \ln\left(\frac{4\eta}{\rho V h}\right) - c + 1/2, \quad (2)$$

with  $c$  Euler's constant. The coefficient  $\alpha$  is of the order of unity in our experiments.

Equation (1) shows that the film bursts at (nearly) constant speed proportional to  $1/\eta_g$ . This is consistent with the quasilinear dynamics already shown in Fig. 2 and is well confirmed in Fig. 4 except for small  $\eta_g$ .

An estimate of the interfacial tension  $\gamma$  between glycerol and oil obtained by the fitting curve in Fig. 4 is reasonable. This is because the estimate of  $\alpha\gamma$  is 7.94 mN/m, which is an appropriate value for the interfacial tension between the glycerol and the oil because  $\alpha$  is of the order of one as pointed out in the above.

The deviation of the data from Eq. (1) for small  $\eta_g$  shown in Fig. 4 can be understood as follows. Velocity gradients are

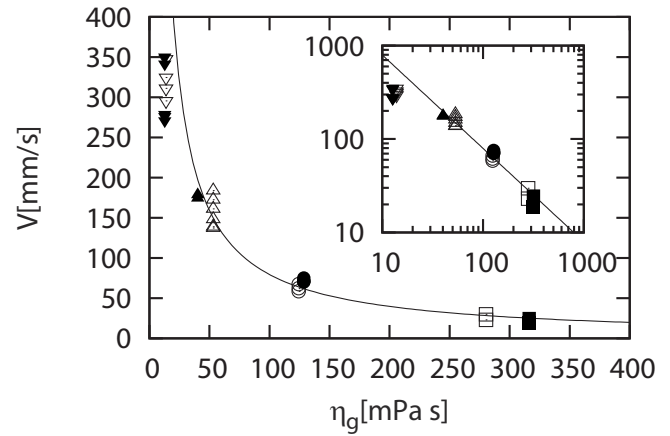


FIG. 4. Bursting speed as a function of glycerol viscosity. The curve in the main plot (or line in the inset) is a fitting curve based on Eq. (1). The data group around  $\eta_g = 10$  mPa s is excluded for this fitting.

created inside the bursting tip of volume around  $h^2D$ :  $V/h$  in the  $r$  direction and  $V/D$  in the direction of cell thickness [the velocity gradient in the film thickness direction is almost zero when  $\eta_g < \eta_o$  and around  $V/h$  when  $\eta_g > \eta_o$ ; see Fig. 3(d) and 3(e)]. This gives the dominant dissipation in the oil film scaling as  $\eta_o V^2 D$  because the thin film thickness is clearly smaller than the cell thickness ( $h < D$ ). This dissipation in the oil film  $\eta_o V^2 D$  becomes comparable to that in the glycerol  $\eta_g V^2 D$  when  $\eta_g$  is decreased and becomes comparable to  $\eta_o$  ( $\approx 60$  mPa s). This is consistent with that the velocities are smaller than the prediction for  $\eta_g$  around 10 mPa s in Fig. 4; the prediction only includes the dissipation in the glycerol and the existence of extra dissipation in the oil makes the velocity smaller. Note that dissipation associated with the escape dynamics illustrated in Fig. 3(c) is negligible because the dynamics is much slower.

The data for  $\eta_g$  around 40–50 mPa s in Fig. 4 follows Eq. (1) although these values are smaller than  $\eta_o$  (but the same order as  $\eta_o$ ). This may be understood if we take into account the exact coefficients neglected in our estimation. The exact coefficient is available for the dissipation in the glycerol at least under the cylinder approximation as quoted in the above, but not for that in the oil. However, the coefficient for the glycerol may be larger than that for the oil (which is consistent with the above behavior) because the volume of the dissipation in the oil may be smaller than in the glycerol: the former is very localized and surrounded by the latter.

The inset of Fig. 2 (together with the main plot at short times) clearly shows the existence of another nonlinear regime at initial times: the bursting proceeds initially not with a constant speed but with faster speeds. The study of this regime is difficult because (1) if we magnify too much the bursting tends to rarely come into view because we cannot predict the starting position of a spontaneous bursting and (2) if we reduce the water content in glycerol to increase the viscosity to slow down the dynamics the viscosity of glycerol becomes inhomogeneous due to high water absorbing property of a dense glycerol. In addition, we cannot interchange the roles of glycerol and oil (where an oil drop sits on a glycerol film) to decrease the viscosity of the glycerol film

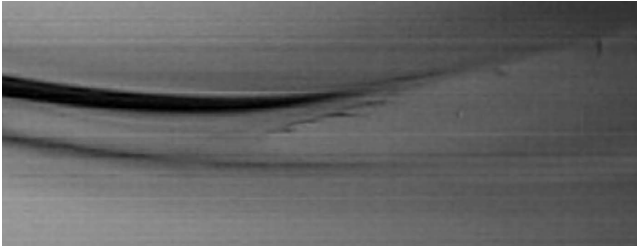


FIG. 5. Instability appearing around a rapidly moving bursting tip.

because the droplet contacts directly with the boards to become too sticky to perform this experiment. Furthermore, if we replace the olive oil with silicone oils, we find rather different dynamics of coalescence probably due to the difference in chemical properties, which will be reported elsewhere [16].

We sometimes observed instability around the bursting tip when  $\eta_g$  is around 10 mPa s, i.e., when the bursting is rapid (see Fig. 5). Similar phenomena are observed also in the nonconfined geometry [10]. As they pointed out the physical origin of these singular shapes may be related to the “selective withdrawal” [17]. This shape is also similar to that of festoons frequently observed on the surface of Jupiter [18] whose physical origin of formation is not well understood.

Thus, this instability is worth studying in the future and may contribute also to the deviation of the data from the prediction of Eq. (1) for small  $\eta_g$ .

In the present work, we study the bursting dynamics of a thin film in a confined geometry. The circular symmetry of the opening hole in bursting films common to the previous studies are broken in our experiment. Even in such a case, the bursting proceeds with a constant velocity, which is consistent with the theory where the viscous dissipation in the surrounding liquid balances with the interfacial drive. However, due to the breaking of the symmetry, any rims are not formed at the bursting tip. The simple understanding of the unusual type of bursting presented here will be indispensable in many modern situations where small amount of liquids should be manipulated. In addition, the present work is quite relevant to understanding the dynamics of droplets, especially the coalescence dynamics of liquids, which has been actively studied [19–27]. In this context, the thinning dynamics of the sandwiched film and mechanism of nucleation of the bursting starting position should be explored, which requires a separate study.

We thank Lorraine Montel for critically reading our manuscript. A.E. is supported by the Japan Society for the Promotion of Science. K.O. thanks the Japanese MEXT for KAKENHI.

- 
- [1] A. Oron, S. H. Davis, and S. G. Bankoff, *Rev. Mod. Phys.* **69**, 931 (1997).
- [2] Special issue edited by G. Reiter and J. Forrest, *Eur. Phys. J. E* **8** (2002).
- [3] G. Reiter, M. Hamieh, P. Damman, S. Slavovs, S. Gabriele, T. Vilmin and E. Raphaël, *Nature Mater.* **4**, 754 (2005).
- [4] P. Damman, S. Gabriele, S. Slavovs, S. Desprez, D. Villers, T. Vilmin, E. Raphaël, M. Hamieh, S. Al Akhrass, and G. Reiter, *Phys. Rev. Lett.* **99**, 036101 (2007).
- [5] P. G. de Gennes, F. Brochard-Wyart, and D. Quéré, *Gouttes, Bulles, Perles et Ondes*, 2nd ed. (Belin, Paris, 2005).
- [6] A. Dupre, *Ann. Chim. Phys.* **11**, 194 (1867).
- [7] F. E. Culick, *J. Appl. Phys.* **31**, 1128 (1960).
- [8] W. R. McEntee and K. J. Mysels, *J. Phys. Chem.* **73**, 3018 (1969).
- [9] C. Redon, F. Brochard-Wyart, and F. Rondelez, *Phys. Rev. Lett.* **66**, 715 (1991).
- [10] É. Reyssat and D. Quéré, *EPL* **76**, 236 (2006).
- [11] G. Debregeas, P. Martin, and F. Brochard-Wyart, *Phys. Rev. Lett.* **75**, 3886 (1995).
- [12] G. Debregeas, P.-G. de Gennes, and F. Brochard-Wyart, *Science* **279**, 1704 (1998).
- [13] The absence of a rim was demonstrated numerically in one-dimensional flow for a purely viscous (i.e., nonviscoelastic) liquid where the bursting speed slows down with time in M. P. Brenner and D. Gueyffier, *Phys. Fluids* **11**, 737 (1999).
- [14] A. Eri and K. Okumura, *Phys. Rev. E* **76**, 060601(R) (2007).
- [15] H. Lamb, *Hydrodynamics* (Cambridge University Press, Cambridge, England, 1974).
- [16] M. Yokota and K. Okumura (unpublished).
- [17] I. Cohen and S. R. Nagel, *Phys. Rev. Lett.* **88**, 074501 (2002).
- [18] J. W. McAnally, *Jupiter and How to Observe It* (Springer, London, 2008).
- [19] P. Constantin, T. F. Dupont, R. E. Goldstein, L. P. Kadanoff, M. J. Shelley, and S. M. Zhou, *Phys. Rev. E* **47**, 4169 (1993).
- [20] J. Eggers, *Rev. Mod. Phys.* **69**, 865 (1997).
- [21] R. E. Goldstein, A. I. Pesci, and M. J. Shelley, *Phys. Rev. Lett.* **75**, 3665 (1995).
- [22] D. Richard, C. Clanet, and D. Quéré, *Nature (London)* **417**, 811 (2002).
- [23] P. Doshi, I. Cohen, W. W. Zhang, M. Siegel, P. Howell, O. A. Basaran, and S. R. Nagel, *Science* **302**, 1185 (2003).
- [24] Y. Couder, S. Protière, E. Fort, and A. Boudaoud, *Nature (London)* **437**, 208 (2005).
- [25] D. G. A. L. Aarts, H. N. W. Lekkerkerker, H. Guo, G. H. Wegdam, and D. Bonn, *Phys. Rev. Lett.* **95**, 164503 (2005).
- [26] J. C. Bird, S. Mandre, and H. A. Stone, *Phys. Rev. Lett.* **100**, 234501 (2008).
- [27] W. D. Ristenpart, J. C. Bird, A. Belmonte, F. Dollar, and H. A. Stone, *Nature (London)* **461**, 377 (2009).